euspen's 25th International Conference & Exhibition, Zaragoza, ES, June 2025
www.euspen.eu

Experimental Analysis of Static, Dynamic, and Thermal Stiffness in Cylindrical Grinder Structures to Investigate Hybrid Application of Cast Iron and Mineral Casting

Taiji Yamada [1], Shun Tanaka [1], Hiroki Otsuka [1], Ryota Kobayashi [1], Shotaro Isoda [1], Naohiko Sugita [1, 2]

[1]*Department of Mechanical Engineering, The University of Tokyo, Tokyo, Japan*
[2]*The Research into Artifacts, Center for Engineering, The University of Tokyo, Tokyo, Japan*

yamada@mfg.t.u-tokyo.ac.jp

Abstract
The mechanical properties of machine tool structural materials significantly influence the static, dynamic, and thermal stiffness, directly impacting machining accuracy. Mineral casting has gained prominence in machine tool bed design as a replacement for cast iron due to its superior damping and thermal stability. Its damping capacity mitigates machine vibrations, enhancing dynamic stiffness, while its thermal stability minimizes the effects of environmental temperature fluctuations and motor-generated heat, thereby reducing structural thermal deformation. However, mineral casting exhibits lower Young's modulus and insufficient strength compared with cast iron. This study aims to enhance the static stiffness, damping properties, and thermal stability of machine tool beds by combining cast iron and mineral casting. Numerical simulations were conducted using FEM (Finite element model/method) to evaluate the static, dynamic, and thermal stiffness of a cylindrical grinder featuring a cast iron bed or a hybrid bed of cast iron and mineral casting designed through topology optimization. Given that the mechanical properties of mineral castings vary based on the manufacturing method, two representative values were used in the analysis. The simulation results were validated against the hammering test vibration data and thermal deformation measurements obtained during no-load operation tests on a cylindrical grinder with a cast iron bed. The geometry obtained through topology optimization suggests where the mineral casting should be placed to enhance each of the three stiffness of the structure. The placement was strongly related to the vibration mode and the location of the heat source. The simulation results demonstrate that the hybrid bed improves the static, dynamic and thermal stiffness by a factor of 0.87-2, revealing a relationship between the material properties of the mineral casting and the stiffness of the structure. These findings confirm the effectiveness of hybrid beds combining cast iron and mineral casting and suggest potential enhancements for machine tool structures.

Finite element analysis (FEM), Grinding, Material, Structure

1. Introduction

The primary role of a machine tool structure is to maintain a constant relative distance between the tool and the workpiece under static, dynamic, and thermal loads during machining [1]. Enhancing the rigidity of the structure is crucial to ensure the accuracy of the machined workpiece.

The design of machine tool structures must consider both geometry and materials. The main structure is typically thin-walled to reduce weight and material costs while maintaining rigidity. Munirathnam investigated ribbed structures to minimize bending displacement [2].

Cast iron and steel plates are commonly used as structural materials, while composite materials such as polymer concrete, granite, ceramic, and fiber-reinforced plastic (FRP) have also been proposed [3,4]. Mineral casting, a type of polymer concrete, has gained attention due to its superior vibration damping performance, thermal stability, and low environmental impact during manufacturing. Mineral casting is a composite material consisting of stone aggregate bonded with epoxy resin [5]. its mechanical properties depend on the particle size of the stone and the content of its ingredients. The relationship between the static, dynamic, and thermal properties of epoxy resin concrete was studied by Kim et al. [6]. Thus, understanding the appropriate material properties is critical for enhancing machine tool performance.

To optimize the design of structural materials and geometry, machine performance must be quantitatively evaluated through simulation. Various approaches have been developed for machine tool analysis. The finite element method (FEM) is widely used for this purpose, while topology optimization [7] is increasingly recognized as a method for structural optimization in the early design phase. Kępczak et al. conducted modal analysis using FEM on a hybrid bed model consisting of a cast iron lathe bed with voids filled with mineral casting, demonstrating improvements in natural frequency [8]. While mineral casting filling is often applied to fill all the voids in a structure, optimizing the amount and areas of filling is essential to maintain lightweight designs and reduce manufacturing costs.

This study aims to determine the optimal material properties and filling regions for mineral casting in cast iron beds. To substantiate the argument that an optimally designed filled bed can substantially enhance the rigidity of the machine tool, the following methodology will be undertaken. A multi-body FEM model was developed to evaluate the deformation of structures subjected to static, dynamic, and thermal loading. This model was further employed to design various mineral casting geometries for filling the cast iron bed through topology optimization. The performance of beds individually optimized for static, dynamic, and thermal stiffness was analyzed by investigating their relationship with the material properties of the mineral casting and the filled volume.

2. Materials and Methods

This section describes the analytical model, conditions used in the study, and the topology optimization method applied to determine the filling geometry.

2.1. FE modeling method

Figure 1 illustrates the 3D model of a cylindrical grinding machine analyzed in this study. The main structural components—such as the bed, traverse table, spindle head, tailstock, and grinding wheel head—are made of cast iron. The bed contains wide voids to reduce weight, which, when filled with mineral casting, are expected to enhance the machine's rigidity. In this study, experimental measurements were conducted on a model with a cast iron bed, and a finite element analysis (FEA) model was developed. A second model was analyzed, where the bed was filled with mineral casting. Alongside the main structure, the model includes components such as the ball screw feed mechanism, wheel spindle, work spindle, drive motors, and the screwdriver. Simplifications were made by omitting covers, accessories, bolt holes, and fillets to reduce computational load. The final model comprises 70 parts and approximately 340,000 mesh nodes.

Table 1 lists the physical properties used in the analysis. Because the mechanical properties of mineral casting depend on the mixing ratio and particle size of the stone, two property sets (MC1 and MC2) were employed. These sets were chosen from a potential range of mineral casting values [9], reflecting its composition as a stone-epoxy resin composite. MC2 represents a higher resin content and displays trends opposite to MC1. As boundary conditions, six-axial spring elements were applied to the bottom of 14 support jacks to replicate floor stiffness. A heat transfer coefficient of 11.2 [W/m·K] was assumed to model heat dissipation from the surface of the structure.

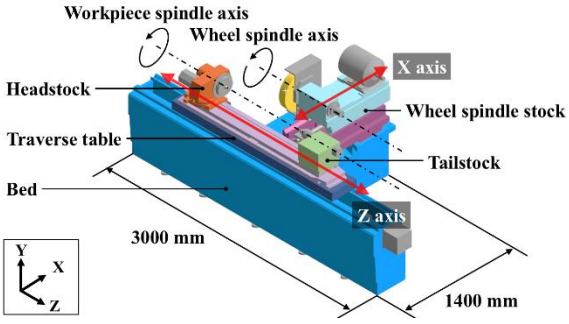

Figure 1. Cylindrical grinding structures

2.2. Topology optimization method

Topology optimization was conducted using Ansys Mechanical 2024 R2 (ANSYS Inc) to determine the optimal configuration of mineral casting within the voids of the bed. Figure 2 highlights the design area analyzed by specifying the percentage of material to be retained. Optimization was performed at fill factors of 25, 50, and 75%, to prioritize areas for filling. The resulting geometries were smoothed using Ansys SpaceClaim 2024 R2 (ANSYS Inc). Separate topology optimizations were conducted for static, dynamic, and thermal stiffness. For static stiffness, the objective was to minimize compliance. For dynamic stiffness, the goal was to maximize the natural frequency of the mode of interest. The target vibration mode had the largest amplitude of bed deformation among experimentally obtained modes provided in Chapter 3. For thermal stiffness, the objective was to minimize thermal compliance.

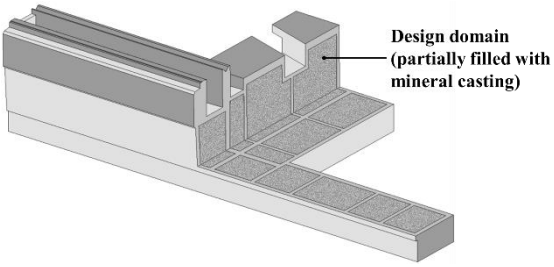

Figure 2. Cross-section of the bed filled with mineral casting

2.3. Analysis method

The inter-axial distance between the grinding wheel axis and the workpiece center axis determines the contour shape of the workpiece. Variations in this distance due to static, dynamic, and thermal loads were analyzed under the conditions described below. The analysis was conducted using Ansys Mechanical 2024 R2 (ANSYS Inc). In the static analysis, gravitational acceleration was applied across the entire model to evaluate the deflection caused by dead weight. Two types of dynamic analyses were performed: modal analysis and frequency response analysis. The frequency response analysis was calculated using the modal superposition method, and the damping ratio for each mode was derived using the half-width method based on experimental values provided in Chapter 3. This study compares the amplitude of inter-axial distance vibrations in modes where deformation of the bed affects this distance, specifically focusing on vibrations along the X-axis. The excitation forces applied were -0.5 N each on the spindle and tailstock and 1 N on the grinding wheel, all along the X-axis direction, simulating grinding resistance. For the thermal analysis, transient heat transfer analysis was employed to evaluate thermal displacement resulting from the rotation of the grinding wheel and spindle. Thermal deformation was calculated based on the temperature distribution within the structure during this process. The motor and bearings of the grinding wheel shaft and spindle were set as heat sources. To maintain the confidentiality of the performance of the machine under consideration, the deformation values obtained from the experiments and analyses described in this manuscript have been normalized.

Table 1. Mechanical properties of materials used in the FEM analysis.

Properties	**Value**			
Material	**Steel**	**Cast iron (FC300)**	**Mineral casting**	
			MC1	**MC2**
Density [kg/m^3]	7800	7310	2400	2100
Young's modulus [GPa]	206	129	35	22
Poisson ratio [-]	0.30	0.25	0.22	0.25
Damping ratio [-]	-	2.7×10^{-4}	2.7×10^{-3}	3.0×10^{-3}
Coefficient of thermal expansion [10^{-6}/K]	11.1	11.0	12.2	20.0
Thermal conductivity [W/m·K]	53.44	45.33	2.00	1.30
Specific heat [J/kg·K]	460.47	460.47	890.00	1100.00

3. Experimental Validation of the Analysis Model

This section outlines the validation of the analytical model through performance tests conducted on a cylindrical grinding machine with a cast iron bed. Experiments were performed on the two items listed below. The results were then compared with those obtained from the analytical model. A performance evaluation, based on the analytical model calibrated using experimental results from the current machine, is conducted in the next chapter.

3.1. Measurement of dynamic properties

The dynamic characteristics of the cylindrical grinder were measured using a hammering test. As illustrated in Figure 3, measurements were conducted with a vibration measurement device manufactured by Ono Sokki Co., Ltd. The machine was vibrated using an impulse hammer (GK-4110G20) in the +X direction of the spindle head, and vibrations were recorded at 48 points on the structure using an accelerometer (NP-3572). The 48 measurement points, shown as black circles in Figure 4, were connected by lines to visualize the mode shapes. The recorded signals were processed with a Fast Fourier Transform (FFT) analyzer (DS-5000) and a signal analysis system called O-solution to generate frequency response functions (FRF). To suppress noise, the FRF was averaged from the results of ten excitation cycles.

Figure 3. Experimental modal analysis setup

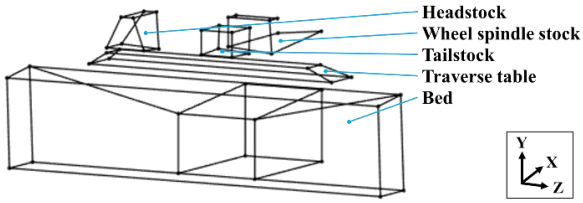

Figure 4. Measurement points for obtaining mode shape

3.2. Measurement of temperature and thermal deformation

The thermal characteristics of the cylindrical grinder were evaluated through a no-load operation test. As depicted in Figure 5, the positions of the grinding wheel spindle, the dummy tool attached to the spindle, and the dummy workpiece in the X-axis direction were measured using an eddy current sensor (EX-305V, Keyence Corp.) fixed to a jig made of Super-invar. The sensor signals were amplified with an amplifier (EX-V01, Keyence Corp.) and recorded using a MEMORY HiCORDER (MR8847A, HIOKI E.E. CORPORATION). Thermal deformation was determined by subtracting the initial position at the start of the measurement from the total displacement recorded. The wheel spindle and work spindle operated continuously for seven hours, during which the displacements were also measured.

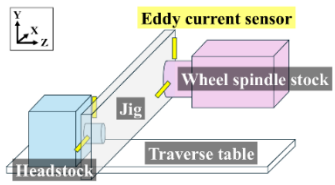

Figure 5. Thermal displacement measurement setup

3.3. Validation of analysis model

As shown in Figure 6, the FRF and vibration modes for the absolute value of spindle head compliance obtained from the hammering test were compared with the simulated results. The seventh-order and higher modes were attributed to structural deformation. Notably, the ninth-order mode, illustrated in Figure 6, exhibited a large amplitude caused by bed deformation. In this mode, the grinding wheel axis and workpiece axis oscillate in phase in the X-axis direction, leading to significant variations in the inter-axial distance. Consequently, the ninth-order mode was selected for optimization. The experimental results closely aligned with the trends observed in the simulation, with a damping ratio of 0.077 obtained for the ninth-order mode. Using this damping ratio, the FEM analysis produced a frequency of 164 Hz, while the experimental results indicated a frequency of 145 Hz, resulting in an error of approximately 13 %. The amplitudes were of the same order. As shown in Figure 6, the vibration modes demonstrated strong agreement between the experiment and simulation.

The measured thermal deformation of the grinding wheel spindle and work spindle during seven hours of no-load operation was compared with the simulated results, as shown in Figure 7. The vertical axis values in Figure 7 are normalized. Both the experimental and simulated results indicated that the wheel spindle tended to elongate in the positive direction due to heat generated by the motor and bearings, while the work spindle elongated in the negative direction as a result of temperature increases caused by heat from the motor and bearings in the headstock.

Therefore, the finite element model accurately captures the predominant characteristics of bed vibrational deformation and thermal expansion, enabling a comprehensive simulation of bed performance.

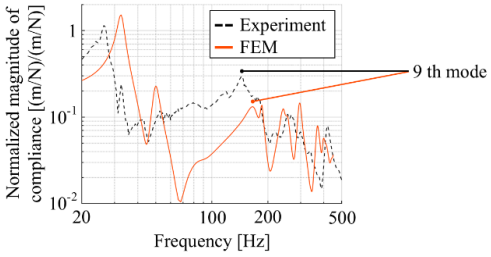

(a) FRF

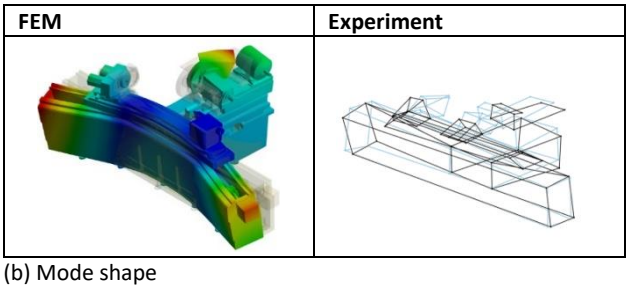

(b) Mode shape

Figure 6. Experimental validation of dynamic characteristics. (a)FRF (b)Mode shape

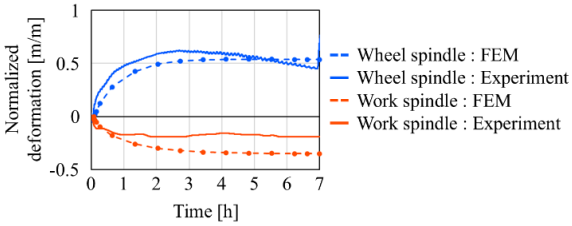

Figure 7. Experimental validation of thermal deformation analysis

4. Results and discussions

This section describes the geometries obtained through topology optimization and the simulated static, dynamic, and thermal stiffnesses for these geometries.

4.1. Optimized structure

Figure 8 illustrates the optimized structure under the conditions of filling with MC1. From left to right, the results for static, dynamic, and thermal analyses are presented. The upper part of the figure shows the optimized geometry in the filling region, with the mass constraints color-coded in blue, red, and green. The lower part provides cross-sectional views of the bed, corresponding to each analysis. The optimized geometry for MC2 exhibited a similar trend.

The coloring of the mass constraints can be interpreted as blue, red, and green, indicating the regions where reinforcement by filling is most effective for static, dynamic and thermal stiffness, respectively. For static stiffness, the fill distribution was almost uniform, starting from the top of the filled area. This tendency to fill from the top is attributed to the pull-out direction specified by manufacturing constraints, which is consistent across all three stiffness properties. For dynamic stiffness, the bed was primarily filled from the center front, reflecting the deformation mode of the central part of the bed that was optimized. For thermal stiffness, the filling began at the rear of the bed and the work spindle head, aligning with the positions of the grinding wheel axis and the work spindle, which are the heat sources.

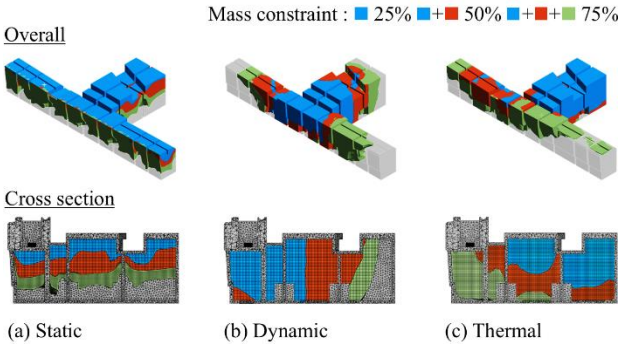

Figure 8. Optimized areas to be filled with mineral casting (MC1)

4.2. Comparison of inter-axial distance

Figure 9 illustrates the relationship between the structure shown in Figure 8 and static, dynamic, and thermal interaxial distance deformations. Inter-axial distance deformation was simulated only for the property being optimized. For instance, static inter-axial distance was calculated exclusively for the model optimized for static stiffness. The calculated deformation values were normalized relative to the deformation of the inter-axial distance at 0% mass constraint, i.e., without filling.

Static deformation decreased up to 50 % as the filling increased. MC2 showed a greater reduction when the filling was minimal, whereas MC1 exhibited a more substantial reduction as the filling increased from 25 % to 50 %. This suggests that at low filling levels, the lightweight MC2 was advantageous due to the significant impact on section modulus improvement. However, as the filling increased, the stiffer MC1 became more favorable once the section modulus approached saturation.

Dynamic deformation initially decreased as the filling increased, reaching a minimum deformation of 65 % at 75 % filling, but subsequently increased as the filling volume grew further. As shown in Figure 8, bed stiffness improved with increasing filling volume at lower levels, but beyond 75 %, the added mass outweighed the stiffness gains, resulting in greater deformation. This trend was observed for both materials, although MC1 demonstrated smaller deformation, indicating that materials with higher Young's modulus are advantageous for dynamic stiffness.

Thermal deformation remained within ±5 % when the filling was less than 75 %, but increased significantly at 100 % filling. This was attributed to the reduced contribution of the bed's physical distance from the heat source and the thermally deformable members in suppressing deformation. When the beds were fully filled, the internal surface area was reduced, significantly decreasing heat dissipation and leading to increased deformation. This trend was consistent across both materials.

To optimize static, dynamic, and thermal stiffness, it is essential to select an appropriate material and determine the optimal filling ratio. The findings of this study suggest that filling 75% of the structure with a high Young's modulus material, such as MC1, enhances static and dynamic stiffness while preserving thermal stiffness. However, this result is derived from individual optimization, and the filling priority may shift when multi-objective optimization is taken into account.

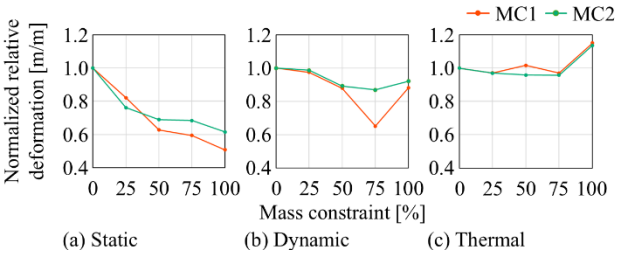

Figure 9. Simulated deformation

5. Conclusions

This study developed a finite element model to estimate the deformation of a cast iron bed structure under static, dynamic, and thermal loading, based on experimental analysis. The model was also used to analytically evaluate the performance of a cast iron bed filled with mineral casting designed using topology optimization, for static, dynamic, and thermal stiffness, respectively. The results demonstrated that deformations were reduced by up to 60 % and highlighted the effectiveness of specific mineral casting material properties and optimized filling locations for each type of load. These findings provide valuable insights for selecting suitable materials and their placement to enhance the static, dynamic, and thermal stiffness of structures through the combined use of cast iron and mineral casting. In this study, performance evaluations of the optimized beds were conducted only for the same parameters used in optimization: static, dynamic, and thermal stiffness. Future work should investigate the impact of prioritizing one of these properties over the others and explore strategies for material arrangement to optimize all three properties simultaneously.

References

[1] Altintas Y 2012 Cambridge university press.
[2] Munirathnam M 2008 Shaker.
[3] Rahman M, Mansur A, and Karim B 2001 *JSME Int. J. Ser. C* **44**(1) 1-11.
[4] Möhring H C, Brecher C, Abele E, Fleischer J, and Blicher F 2015 *CIRP annals* **64**(2) 725-748.
[5] Mineral casting (EPUMENT). https://www.rampf-group.com/en/products-solutions/details/mineral-casting-epument/. Accessed 8 January 2025.
[6] Kim H S, Park K Y and Lee D G 1995 *J. Mater. Process. Technol.* **48**(1-4) 649-655.
[7] Chan T C, Chang C C, Ullah A, and Lin H H 2023 *Appl. Sci.* **13**(8) 4742.
[8] Kępczak N, Pawlowski W, and Kaczmarek Ł 2015 *Arch. Metall. Mater.* **60**(2) 1023-1029.
[9] Kępczak N and Pawlowski W 2013 *Mech. Mech. Eng.* **17**(3) 5-15.